

RESEARCH

Open Access



Short and Long RC Columns with Internal WWM Reinforcement under Concentric and Eccentric Compression

Ahmed M. El-Kholy^{1*} , Safaa F. Abd El-Rahman^{1,2} and Mohamed M. El-Assaly¹

Abstract

Recently, various types of steel meshes were used as additional internal reinforcement for improving the confinement, ductility, and strength of the reinforced concrete (RC) columns. In this experimental study, a welded wire mesh (WWM) layer was used as an internal reinforcement in addition to the traditional steel reinforcement (longitudinal bars and transverse ties) for short and long RC columns under concentric and eccentric compression. Thirty-six square RC columns with two slenderness ratios λ (height to width ratio) of 9 and 18 were tested under compression with eccentricity ratios e/t (eccentricity to section thickness ratio) of 0, 0.13, and 0.26. The reference columns were traditionally reinforced with longitudinal steel bars and transverse ties with a reference volumetric ratio ρ_r of 0.44%. The other columns comprised a WWM layer wrapped outside the ties whose volumetric ratio ranged from 0.22% to 0.44%. The results demonstrated that the columns reinforced with a WWM layer in addition to traditional reinforcement showed an improvement in ductility and strength compared to those reinforced with longitudinal bars and transverse ties only. A WWM layer increased the ultimate load of the columns comprising ρ_r ties by approximately 16% and 9% for short and long columns, respectively. These improvements were proportional to the ties volumetric ratio.

Keywords: Short RC columns, Long (slender) RC columns, Concentric compression, Eccentric compression, Confinement, Steel meshes (WWM), Ties

1 Introduction

The failure of RC columns is brittle and may lead to the collapse of the structure. In reality, there are no columns subjected to a fully concentric compression because of the curtailment of column cross section in higher floors, and the construction tolerance, or the existence of explicit eccentric loads. The columns subjected to eccentric compression are susceptible to normal force and bending moment. While the eccentricity increases, the ultimate load and the axial deflection of the column decrease but the lateral deflection increases (Widiarsa

& Hadi 2013). There are two types of RC columns; short and long (slender) columns. Long columns are frequently used in unconventional structures. The column is categorized as either short or long according to its slenderness ratio (λ) which is the height to width ratio (for square and rectangular columns) multiplied by a unit factor for simply supported columns (Egyptian code committee for concrete structures 2018). For braced RC structures, the Egyptian code for the design and construction of concrete structures categorizes the square (or rectangular) column as short or long (slender) if its λ is smaller than 15 or ranges from 15 to 30, respectively. Long columns are susceptible to overall buckling and additional moments due to their high slenderness ratio. An alternative definition for λ as the ratio between the height and the radius of gyration existed in both the Egyptian code and ACI318

Journal information: ISSN 1976-0485 / eISSN 2234-1315

*Correspondence: amk00@fayoum.edu.eg; ahmed.elkholy@fayoum.edu.eg

¹ Civil Engineering Department, Faculty of Engineering, Fayoum University, Kiman Fares, El-Fayoum, Egypt

Full list of author information is available at the end of the article



© The Author(s) 2022. **Open Access** This article is licensed under a Creative Commons Attribution 4.0 International License, which permits use, sharing, adaptation, distribution and reproduction in any medium or format, as long as you give appropriate credit to the original author(s) and the source, provide a link to the Creative Commons licence, and indicate if changes were made. The images or other third party material in this article are included in the article's Creative Commons licence, unless indicated otherwise in a credit line to the material. If material is not included in the article's Creative Commons licence and your intended use is not permitted by statutory regulation or exceeds the permitted use, you will need to obtain permission directly from the copyright holder. To view a copy of this licence, visit <http://creativecommons.org/licenses/by/4.0/>.

code (ACI318 committee 2014). Both the alternatives are identical. However, the second one (height to the radius of gyration ratio) results in mathematically $\sqrt{12}$ times the values of the first definition (height to width ratio; used in this paper) in case of square columns, and therefore, λ limits for slender columns are different for each definition.

The traditional reinforcement of RC columns comprises longitudinal steel bars and transverse steel ties. The longitudinal reinforcement contributes to the axial strength of RC columns, and also improves the flexural strength of eccentric RC columns by acting as tensile and compressive reinforcements on the two faces (of the column) subjected to extreme flexural deformation. The transverse reinforcement contributes to the axial strength of RC columns by improving the concrete confinement which is proportional to the volumetric ratio ρ of transverse ties as long as the continuity between the concrete core and cover is preserved.

Recently, steel meshes such as welded wire mesh (WWM), expanded metal mesh (EMM), hexagonal chicken wire mesh, and biaxial geogrid have been used as an internal reinforcement in addition to the traditional reinforcement to improve the confinement and strength of RC columns (Bastami et al. 2022; Daou et al. 2020; El-Kholy & Dahish 2015; El-Kholy et al. 2018). For existing columns, the steel meshes (in a form of ferrocement) was externally used as an additional reinforcement (El-Kholy et al. 2019a; Ganesan & Anil 1993; Kaish et al. 2018) or alternatively, fiber reinforced polymers (FRP) sheets have been externally bonded to RC columns (Choi et al. 2021; El-Kholy et al. 2022; Hashemi et al. 2022; Siddiqui et al. 2020). The longitudinal wires of WWM, and the FRP sheets aligned in the longitudinal direction act similar to the traditional longitudinal steel bars in improving the axial and flexural strengths of RC columns. In addition, the transverse wires of WWM, and the FRP sheets aligned in the transverse direction act similar to the traditional transverse steel ties in improving the confinement and the axial strengths of RC columns. The confinement effectiveness in enhancing the column strength is reduced with the increase in either the eccentricity (Xing et al. 2020; El Maaddawy 2009) or the slenderness ratio (El Maaddawy 2009; Pan et al. 2007). Thus, the confinement effectiveness produced by transverse reinforcement is more relevant for short columns especially if they are loaded concentrically (minor eccentricity is inevitable). Conversely, the flexural strength produced by the cross-sectional lateral rigidity and the longitudinal reinforcement is more relevant for long and eccentrically loaded columns.

For short columns under concentric compression, many studies investigated the additional reinforcement of

internal steel meshes. El-Kholy and Danish (2015) tested twelve square RC columns ($\lambda=7.3$ and $14 - \rho=0.05-0.27\%$) comprising an EMM layer wrapped outside the traditional reinforcement. For the columns comprising ρ of 0.27%, the EMM layer increased the load capacity with average of 14.79%. This improvement in ultimate load was reduced with decreasing ρ . Tahir et al. (2017) tested six square columns ($\lambda=4.9 - \rho=0.76\%$) comprising an EMM layer wrapped either inside or outside the traditional reinforcement. The EMM layer increased the average load capacity with 10.25% and 17.93% for inside and outside configurations, respectively, over the reference columns whose ρ was 1.37%. El-Kholy et al. (2018) investigated 26 square columns ($\lambda=7.3 - \rho=0-0.33\%$) comprising either WWM or EMM meshes (1 or 2 layers) wrapped outside the traditional reinforcement, and showed that the effectiveness of WWM outperformed that of EMM. The WWM layer increased the average load capacity with 32.33%, and 18.92% in case of $\rho=0.17-0.33\%$, and zero ties, respectively, over the reference columns whose ρ was 0.33%. El-Kholy et al. (2018) recommended optimum reinforcement of one WWM layer and ties with $\rho=0.17\%$, and showed the effectiveness of the steel meshes for heat-damaged columns too. Razvi and Shaikh (2018) investigated six square columns ($\lambda=6.4 - \rho=0$ and 0.57%) comprising a WWM layer and compared the results with the reference columns comprising $\rho=0.57\%$. The WWM layer increased the average load capacity with 20.82% and 0.91% in case of $\rho=0.57\%$ and zero ties, respectively. Emara et al. (2021) presented the full and partial wrapping of EMM (single and double layers) as an additional reinforcement for twelve engineered cementitious composite circular columns ($\lambda=5 - \rho=zero$ and 0.56%), and compared their behavior with the reference columns comprising $\rho=0.56\%$. For fibers content of 1.5%, the EMM additional reinforcement increased the average load capacity with 13.25%, 10.92%, and 7.27% in case of full wrapping with $\rho=0.56\%$, full wrapping with zero ties, and partial wrapping with $\rho=0.56\%$, respectively. Not only internal steel meshes, but also external FRP transverse sheets were frequently used as additional reinforcement for short columns under concentric compression. Raval and Dave (2013) added a FRP sheet layer to six columns of circular, square, and rectangular cross sections ($\lambda=5.9, 6.7, and 9.1, respectively$), and comprising average ρ of 0.62%. The FRP layer increased the average load capacity with 159%, 79%, and 76% for circular, square, and rectangular columns compared with the references. In addition, Vesmawala and Kodag (2017) added a FRP sheet layer to nine columns of circular, square, and, rectangular cross sections ($\lambda=4.1, 4.7, and 8.8, respectively$), and comprising average ρ of 0.28%. The FRP layer increased the

average load capacity with 73%, 101%, and 106% for circular, square, and rectangular columns compared with the references. Ghanem and Harik (2018) numerically investigated the partial wrapping of FRP strips for circular columns ($\lambda=3$ — $\rho=0.4$ and 0.64%), and concluded that increasing the number of FRP strips improves the ultimate compressive stress. In addition, it was proved the effectiveness of full wrapping for improving the ultimate compressive stress over the partial wrapping. Al-Nimry and Ghanem (2017) investigated adding one and two FRP sheet layers for twelve heat-damaged circular columns ($\lambda=4.7$ — $\rho=0.4\%$), and concluded that two layers of carbon FRP could restore and even exceed the original strength of the reference unheated columns but failed to reinstate their original stiffness. In all the previously presented studies, the additional reinforcement (either steel meshes or FRP transverse sheets) increased the plastic deformation and the ductility of RC columns.

For short columns under eccentric compression, only Hadi and Zhao (2011) investigated the steel meshes as an additional internal reinforcement. Hadi and Zhao (2011) tested nine circular high strength concrete columns ($\lambda=4.5$ — helix ties) comprising single layer of different types of steel meshes (aluminum fly, WWM, and fiberglass fly) under eccentric compression (eccentricity ratio e/t =zero, 0.12, and 0.24). The eccentricity ratio is the ratio of the eccentricity e to the section thickness t . Hadi and Zhao (2011) showed that the WWM outperformed the aluminum fly, and fiberglass fly meshes in terms of the effectiveness in improving the ultimate load capacity. The WWM layer increased the load capacity with 13.05%, 4.93%, and 31.15% in case of e/t =zero, 0.12, and 0.24, respectively, compared with the reference columns (without any steel meshes). Despite only one study (Hadi & Zhao 2011) investigated the steel meshes as an additional internal reinforcement for short columns under eccentric compression, many studies investigated the FRP longitudinal and transverse sheets as an additional external reinforcement for these columns. Sample three studies are briefly presented. Al-Nimry and Al-Rabadi (2019) installed a transverse FRP sheet layer or a longitudinal FRP sheet layer coupled with a transverse FRP sheet layer for twenty circular columns ($\lambda=6.3$ — $\rho=0.13$ – 0.26% — $e/t=0.13$ – 0.34), and concluded that the effectiveness of the longitudinal layer wrapped with a hoop layer outperformed that of single hoop layer in terms of the ultimate load capacity. Quiertant and Clement (2011) investigated different types and configurations of a combined FRP reinforcement consisting of longitudinal sheets or plates (aligned in different orientations) coupled with a transverse FRP sheet layer (continuous or discontinuous wrapping) for eight square columns ($\lambda=12.5$ — $\rho=0.17\%$ — $e/t=0.10$), and maximum achievement

in the ultimate load capacity was 30.31%. Siddiqui et al. (2020) installed longitudinal FRP sheets (2, and 4 layers) and/or a transverse FRP sheet layer for nine square columns ($\lambda=4$ – 8 — $\rho=0.50\%$ — $e/t=0.17$), and could achieve approximately 150% increment in ultimate load capacity in case of 4 FRP layers.

For long columns under either concentric or eccentric compression, no studies investigated using the steel meshes as an additional internal reinforcement. Conversely, few studies investigated using the FRP longitudinal and transverse sheets as an additional external reinforcement of RC long columns. Sample four studies (two under concentric compression and two under eccentric compression) are briefly presented. Pan et al. (2007) tested and simulated six rectangular columns ($\lambda=4.5$ – 17.5 — $\rho=0.48\%$) with additional reinforcement of a transverse FRP sheet layer under concentric compression, and showed that the effectiveness of the external FRP reinforcement decreases with the increase of slenderness ratio. El-Kholy et al. (2022) simulated 58 square and rectangular columns ($\lambda=15$ – 35 — $\rho=0.37$ – 0.49%) with additional reinforcement of 1–4 longitudinal FRP sheet layers (full or partial coverage of column height) and/or one transverse FRP sheet layer under concentric compression. El-Kholy et al. (2022) recommended using the longitudinal FRP sheets for $\lambda=15$ – 22 , and the partial longitudinal FRP sheets for $\lambda>22$. Gajdosova and Bilcik (2013) tested 6 rectangular columns ($\lambda=27.3$ — $\rho=0.39\%$) with additional reinforcement of near surface mounted (NSM) FRP strips in the longitudinal direction or a transverse FRP sheet layer under eccentric compression ($e/t=0.27$). The effectiveness of NSM FRP strips outperformed that of transverse sheet layer in terms of ultimate load improvement. Moreover, Gajdosova and Bilcik (2013) recommended using NSM FRP longitudinal strips for $\lambda>16$ based on numerical parametric study. Si Youcef et al. (2015a, b) tested nine square columns ($\lambda=13$ – 23.6 — $\rho=0.11$ – 0.17%) with additional reinforcement of FRP sheets (1, 2 layers) installed in the transverse, longitudinal and inclined (45°) directions (with different combinations) under double eccentricity compression ($e/t=0.30$ – 0.55). Si Youcef et al. (2015a, b) showed that the most effective reinforcement pattern for slender columns under eccentric compression was the longitudinal sheets wrapped with a transverse sheet, followed by the longitudinal sheets, then the inclined sheets, and finally the transverse sheets.

Based on the introduced literature review, the following three limitations could be concluded. First, no studies investigated the long columns with additional reinforcement of internal WWM under either concentric or eccentric compression. Second, only one study (Hadi & Zhao 2011) investigated the short columns with

additional reinforcement of internal WWM under eccentric compression. Third, a few studies investigated the short columns with additional reinforcement of internal WWM under only concentric compression (El-Kholy & Dahish 2015; El-Kholy et al. 2018; Razvi & Shaikh 2018; Tahir et al. 2017). These limitations motivated the authors to present the current study. In this paper, 36 RC square columns (eighteen short columns of $\lambda=9$, and eighteen slender columns of $\lambda=18$) comprising a traditional steel reinforcement with different ρ (0.44% and 0.22%) and an additional reinforcement of one internal WWM layer were tested under concentric and eccentric compression ($e/t=0, 0.13, \text{ and } 0.26$).

2 Experimental Program

In this study, 36 square RC columns with cross-sectional thickness $t=115 \text{ mm}$ and two different slenderness ratios ($\lambda=9$ and 18) were cast in the concrete research and material properties laboratory at Fayoum University. The reinforcement of the columns consisted of longitudinal bars, transverse ties ($\rho=0.44\%$ and 0.22%), and an internal WWM layer. Table 1 shows the testing scheme. The columns specimens were tested under concentric

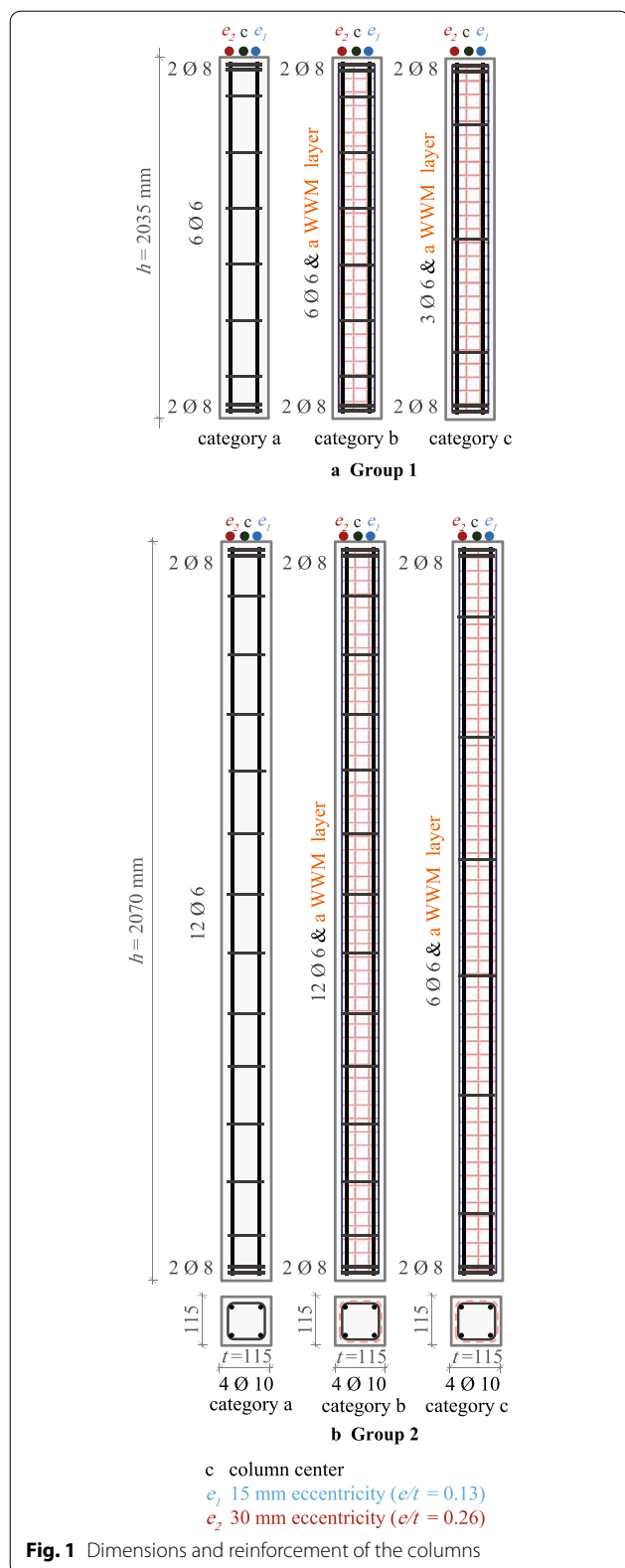
and eccentric compression ($e/t=0, 0.13$ and 0.26) in the structural laboratory at the American University in Cairo (AUC). The columns were divided into two groups (Fig. 1) according to the slenderness ratio. The first group contained eighteen columns of 1035 mm height ($\lambda=9$), whereas the second group contained eighteen columns of 2070 mm height ($\lambda=18$). Each group was divided into three categories (a, b and c) based on the volumetric ratio of ties ($\rho=0.44\%$ or 0.22%) and the additional internal reinforcement (a WWM layer or nil). Fig. 1 and 2 show the details of the specimens for the three categories. Category a comprised the reference columns with traditional steel reinforcement of four longitudinal bars, and ties of $\rho_r=0.44\%$ ratio. Category b columns comprised the same traditional steel reinforcement in addition to internal reinforcement of a WWM layer. Category c columns comprised the same traditional steel reinforcement but ties was reduced to $0.5\rho_r$ ($\rho=0.22\%$) in addition to internal reinforcement of a WWM layer. Each category comprised six columns (3 identical pairs). The first pair was tested under concentric load, whereas the second and third pairs were tested under eccentricities of 15 mm ($e/t=0.13$) and 30 mm ($e/t=0.26$), respectively.

Table 1 ID, dimensions and reinforcement of tested column specimens

Group	Category	Specimen ID ^a	Repetition	Eccentricity e (mm)	Dimensions $t \times t \times h$ (mm)	Reinforcement													
						Vertical bars ^b grade (360/520)	Ties ^b grade (240/350)	Ties volumetric ratio ρ %	Additional internal reinforcement										
1	a	S6R0	2	0	$115 \times 115 \times 1035$	$4 \text{ } \emptyset 10$	$6 \text{ } \emptyset 6$	0.44	–										
		S6R15	2	15															
		S6R30	2	30															
	b	S6W0	2	0						$115 \times 115 \times 1035$	$4 \text{ } \emptyset 10$	$6 \text{ } \emptyset 6$	0.44	a WWM layer					
		S6W15	2	15															
		S6W30	2	30															
	c	S3W0	2	0											$115 \times 115 \times 1035$	$4 \text{ } \emptyset 10$	$3 \text{ } \emptyset 6$	0.22	a WWM layer
		S3W15	2	15															
		S3W30	2	30															
2	a	L12R0	2	0	$115 \times 115 \times 2070$	$4 \text{ } \emptyset 10$	$12 \text{ } \emptyset 6$	0.44	–										
		L12R15	2	15															
		L12R30	2	30															
	b	L12W0	2	0						$115 \times 115 \times 2070$	$4 \text{ } \emptyset 10$	$12 \text{ } \emptyset 6$	0.44	a WWM layer					
		L12W15	2	15															
		L12W30	2	30															
	c	L6W0	2	0											$115 \times 115 \times 2070$	$4 \text{ } \emptyset 10$	$6 \text{ } \emptyset 6$	0.22	a WWM layer
		L6W15	2	15															
		L6W30	2	30															

^a The first and second numbers in the ID refer to the total number of ties per column and the eccentricity value (e mm), respectively. S, L, R, and W refer to short, long, reference and WWM, respectively

^b $x \text{ } \emptyset y$ indicates x bars (or ties) of diameter y mm



2.1 Material Properties

425 kg of Portland cement (CEMI 42.5 N), 204 kg of fresh water, 1183 kg of coarse aggregate (basalt mix of sizes 10 mm and 20 mm), and 599 kg of natural siliceous fine sand were used to cast one cubic meter of concrete. The water–cement ratio was 0.48 by weight of cement. The aggregates were almost impurity-free and free of organic content. The slump of fresh concrete was 65 mm. The concrete compressive strength at 7 and 28 days were 29.7 and 37.7 MPa, respectively, based on the average results of standard 150 mm cubes. The longitudinal reinforcement was high-grade steel (360/520) of 10 mm diameter, whereas the transverse ties reinforcement was mild steel (grade 240/350) of 6 mm diameter. The properties of coarse aggregate, fine aggregate, reinforcement steel are listed in Tables 2, 3 and 4 respectively. Two wires of the used WWM were tested under uniaxial tension in the AUC Mechanical laboratory. Fig. 3 depicts the testing and the average stress–strain curve of tested WWM wires. Table 5 shows the WWM properties. More details about the specimens, testing procedures, and results of the material tests are available in Abd El-Rahman (2022). The testing procedures of all materials and the qualities of all materials were in accordance with the Egyptian Standards (2008, 2009, 2015a, b) and the Egyptian code for concrete structures (2018).

2.2 Specimens Preparation

2.2.1 Steel Reinforcement

All columns were longitudinally reinforced with four bars of 10 mm diameter. In both categories a and b, six ties (6 mm diameter) per longitudinal meter ($\rho = \rho_r = 0.44\%$) were utilized, whereas only three ties per longitudinal meter ($\rho = 0.22\%$) were utilized in category c. To eliminate the local failure of the specimen ends during loading, two ties of 8 mm diameter were used at both ends of all columns. The WWM sheets were cut into pieces with a length of the tie perimeter in addition to an overlapping length of 50 mm. The WWM sheets were too stiff to bend by hands. Therefore, they were molded by a bending machine to be wrapped on the outside perimeter of the ties. Figs. 1, 2 and Table 1 present the reinforcement details.

2.2.2 Wooden Formwork

Fig. 4 shows the wooden formwork (50 mm thickness) prepared to cast the long columns. The base dimensions were 1865 mm \times 2170 mm with height of 120 mm. The same formwork was used to cast the short columns

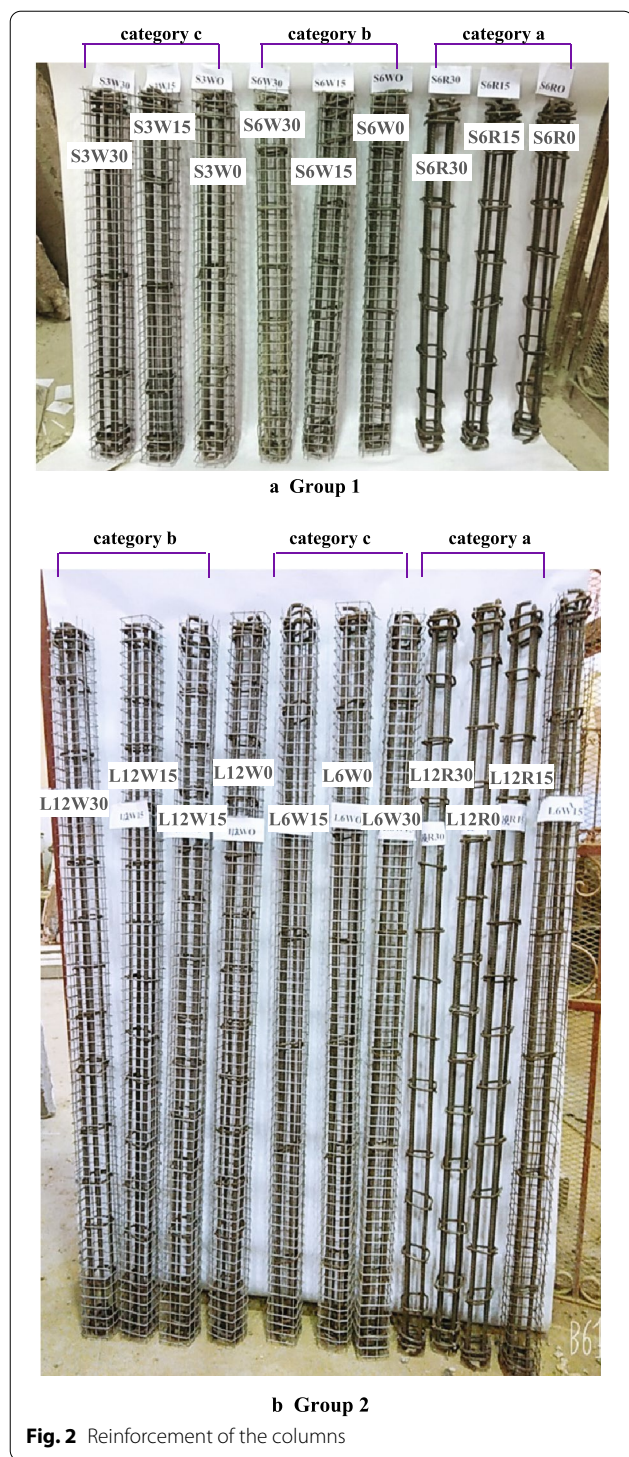


Fig. 2 Reinforcement of the columns

by adding thick wooden pieces (50 mm thickness) at 1035 mm from the formwork face. For preserving the samples surface, the inner faces of formworks were coated with Zetolan SH2 (CMB 2013).

Table 2 Properties of coarse aggregate

Property	Value
Maximum aggregate size (mm)	16
Specific gravity	2.8
Absorption	2%
Bulk density (kg/m ³)	1490
Crushing strength	27%

For more details on specimens and test procedures, refer to Abd El-Rahman (2022), the Egyptian Standards (2008), and the Egyptian code for concrete structures (2018)

Table 3 Properties of fine aggregate

Property	Value
Fineness modulus	2.44
Specific gravity	2.53
Absorption	1.6%
Bulk density (kg/m ³)	1640
Percentage of clay and other fine materials	1.5%
Percentage of chlorides	0.014
percentage of sulphates	0.213

For more details on specimens and test procedures, refer to Abd El-Rahman (2022), the Egyptian Standards (2008), and the Egyptian code for concrete structures (2018)

Table 4 Properties of traditional steel reinforcement

Property	Grade (360/520)	Grade (240/350)
Ultimate stress (MPa)	563	412
Proof stress (MPa)	367	296
Elongation	12%	22%

For more details on specimens and test procedures, refer to Abd El-Rahman (2022), the Egyptian Standards (2015a, b), and the Egyptian code for concrete structures (2018)

2.2.3 Specimens Casting and Curing

The concrete mix components were mixed for 4 min by an electrical mixer, and then the fresh concrete was poured into the formworks, as shown in Fig. 5. After 24 h, the specimens were covered with burlap, and they were cured with tap water, as shown in Fig. 6. After 28 days, the specimens were uncovered to completely dry (Fig. 7) before testing.

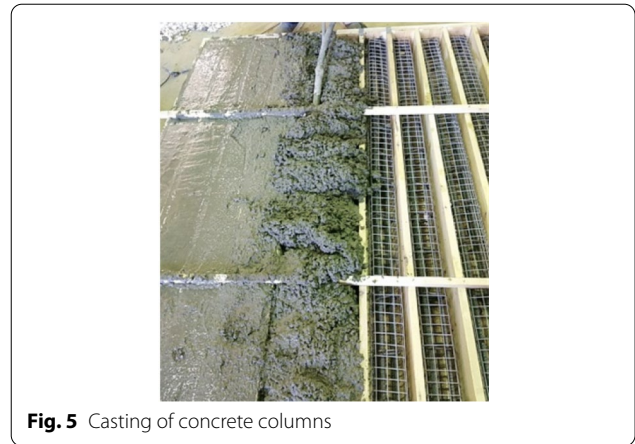
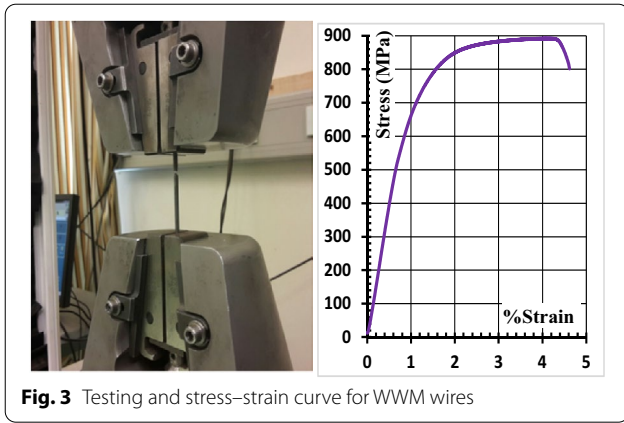


Table 5 Properties of WWM mesh

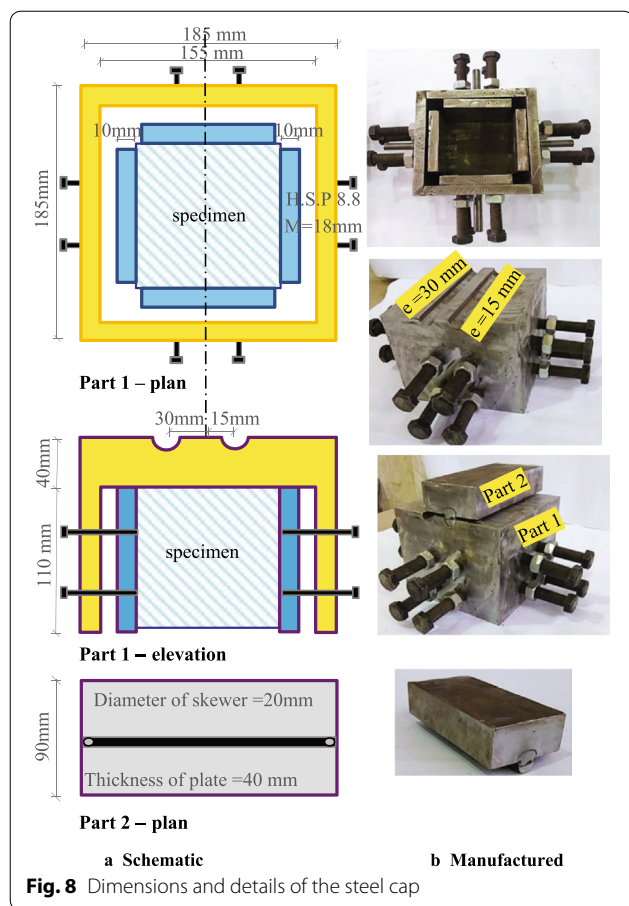
The property	WWM
Opening dimension (mm)	30 × 30
Wire dimension (mm)	2.5
Weight (kg/m ²)	2.58
Proof stress (MPa)	670
Ultimate stress (MPa)	891
Specific gravity	6.5



2.2.4 Instrumentation and Testing

The ENERPAC 3000 kN testing machine was used to test all the specimens. To apply eccentricity, two rigid caps were used at the two ends of each specimen. Each cap consists of two parts. Part 1 is an iron anthropomorphic of a cross section of 185 mm × 185 mm and a height of 150 mm. Part 2 is an iron plate (185 mm × 90 mm × 40 mm) with a skewer of 20 mm diameter at the plate center. On each side of part 1, there is a plate with a thickness of 10 mm welded to four

high strength bolts (18 mm diameter) to achieve sufficient confinement for the column ends. Dimensions and details of the cap are shown in Fig. 8. The test setup is shown in Fig. 9. Two displacement transducers (LVDT)



were mounted to each specimen to determine the axial and lateral displacements. The first LVDT was vertically placed at the bottom face of a steel angle which was fixed in the column center at its top end. The second LVDT was placed perpendicular to the tension face at the mid-point of the column height. The axial strain was monitored on the concrete surface at mid-height of the compression and tension faces for only three sample columns (S6R30, L12R30, and L6W30) that were tested under the same 30 mm eccentricity ($e/t=0.26$).

3 Experimental Results

The ultimate load values are given in Table 6 for the tested columns specimens. Fig. 10 shows the load–axial displacement and load–lateral displacement histories for the tested column specimens. Fig. 11 illustrates the increment in ultimate load for the columns of categories b and c compared with the corresponding reference columns in category a. Figs. 12 and 13 present the axial and lateral displacements, respectively, at the ultimate load for all columns. The lateral displacements for the columns tested under concentric load in group 1 (S6R0, S6W0, and S3W0) were not measured, because it was expected

that the lateral deformations were close to zero for those short columns under concentric load. Fig. 14 presents the energy absorption for all tested columns. Fig. 15 illustrates the relationship between the vertical load and the axial strain on the tension and compression faces of sample three columns; L12R30, L6W30, and S3W30. Fig. 16 illustrates the failure patterns of the tested columns.

3.1 Ultimate Load

Fig. 11 demonstrates that all the columns comprising an internal reinforcement of a WWM layer (in addition to steel ties with a volumetric ratio of either ρ_r or $0.5\rho_r$) sustained a higher ultimate load than the reference columns that comprised ties of ρ_r ratio and no WWM layers. In addition, the increment in ultimate load was more significant for group 1 (short columns) than group 2 (long columns). Fig. 11 reveals that adding one layer of WWM as internal reinforcement to a reference transverse ties ($\rho_r=0.44$) increased the average ultimate load by 15% and 8% for the short and long columns, respectively, compared with the corresponding reference columns. Reducing ρ_r to $0.5\rho_r$ decreased the previous average increments in ultimate load to 7% and 4% for group 1 and group 2, respectively. Thus, the average increment in ultimate load for ρ_r and $0.5\rho_r$ columns together was 11% and 6% for group 1 and group 2, respectively, compared with reference columns. This means that doubling λ , approximately reduces half the increment in the ultimate load. In addition, reducing ρ_r to $0.5\rho_r$, approximately reduced the ultimate load increment to the half for the same λ . In other words, the synergistic effectiveness of ρ_r ties ensured by a WWM layer (category b) was 2.1 times that of $0.5\rho_r$ ties ensured by a WWM layer (category c).

The eccentricity effect on the improvement in the ultimate load (due to adding WWM) is clear in Fig. 11. The WWM effectiveness clearly appeared for concentrically loaded columns in both groups, and its contribution to the increment in ultimate load decreased with the increase of the eccentricity ratio. The average increment (due to adding a WWM layer) in ultimate load for the columns tested under concentric load was 11%, whereas the corresponding increments for the columns tested under eccentric load were 10% and 6% for eccentricity ratios 0.13 and 0.26, respectively. In other words, the average increment in ultimate load for the columns tested under eccentricity ratio 0.26 was approximately 0.54 times that of the columns tested under concentric load.

For the same category (identical ties, identical existence of WWM or not, and identical slenderness ratio), the eccentricity effect on reducing the ultimate load value could be estimated using the ultimate load values given in Table 6. In each category, the first column could

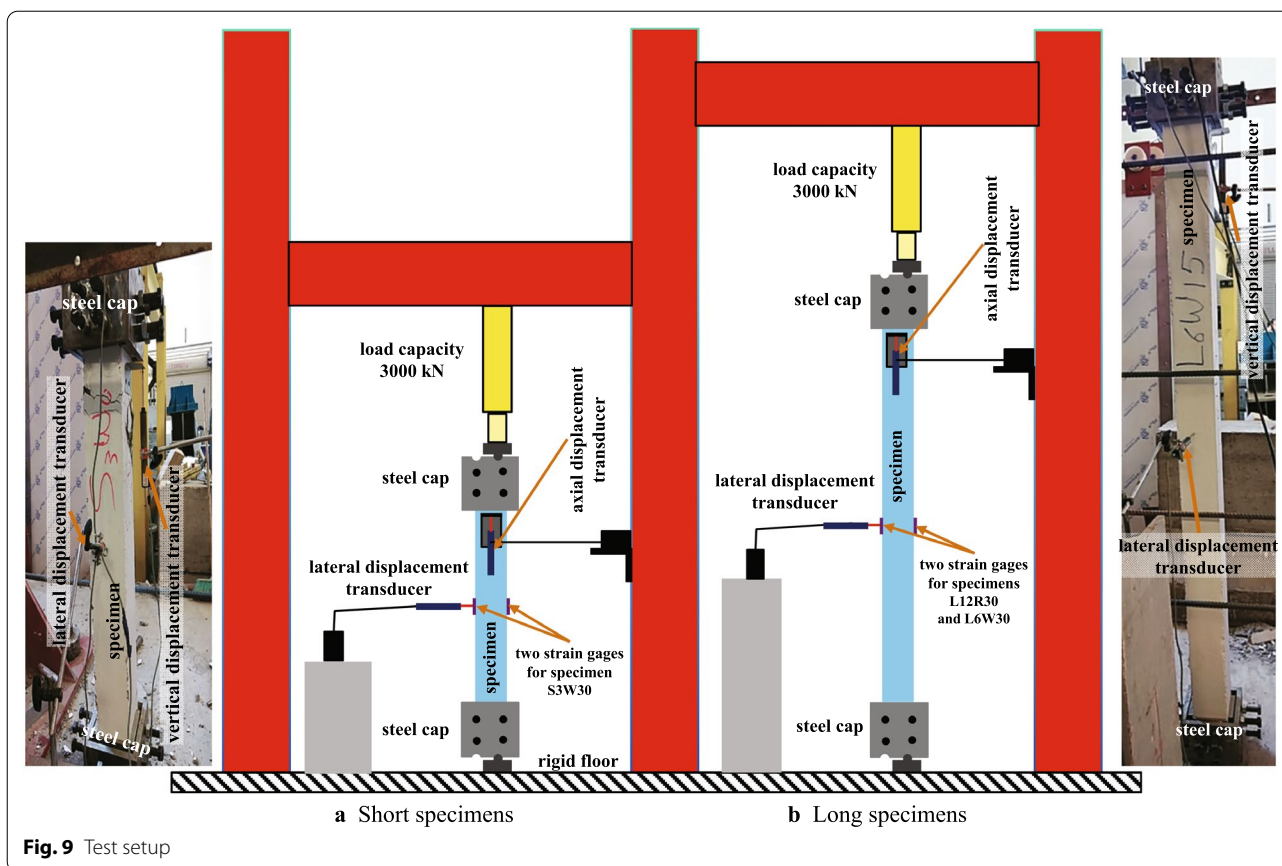


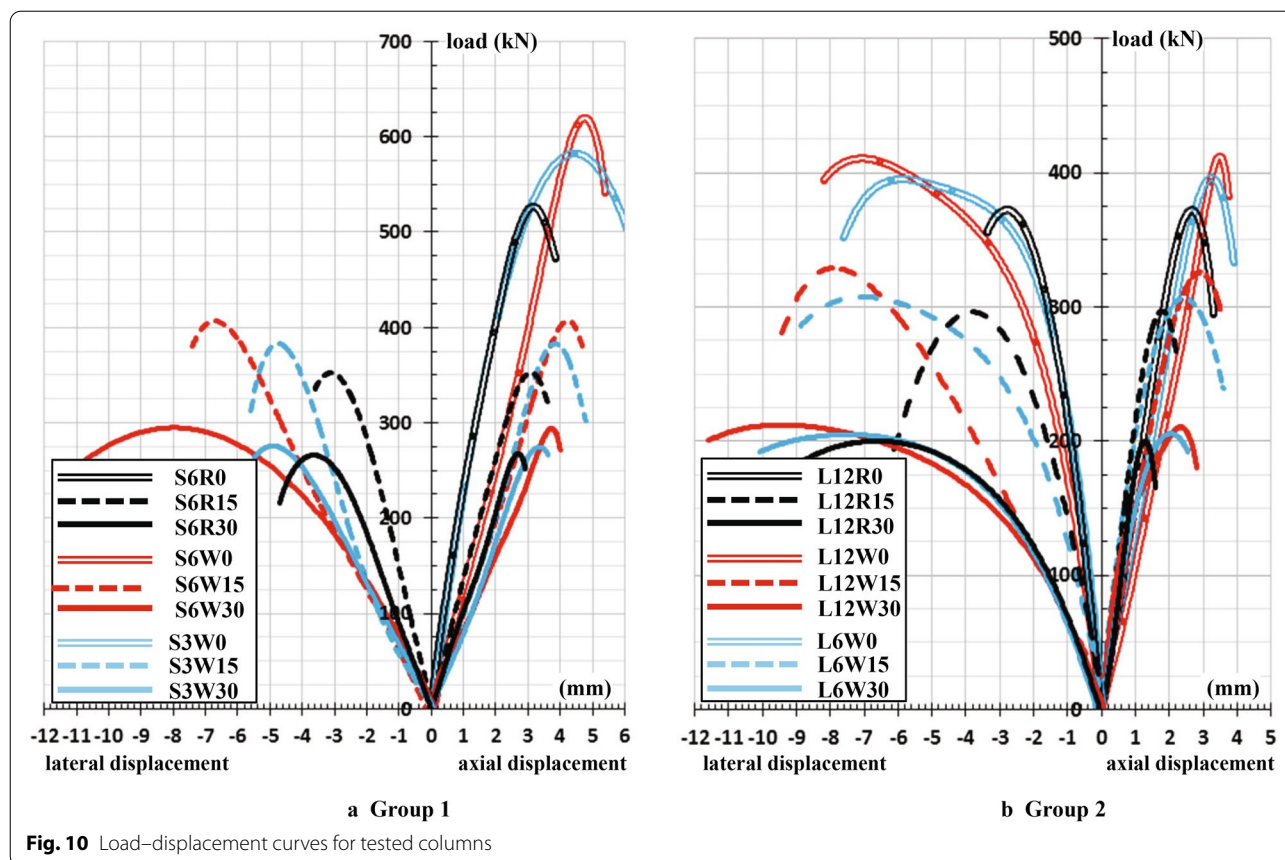
Fig. 9 Test setup

Table 6 Results of tested column specimens

Group	Category	Specimen ID	Ultimate load	
			(kN)	+ %
1	a	S6R0	525.10	–
		S6R15	350.03	–
		S6R30	266.99	–
	b	S6W0	620.94	18.25
		S6W15	406.68	16.18
		S6W30	295.97	10.85
	c	S3W0	578.82	10.23
		S3W15	381.12	8.88
		S3W30	275.10	3.04
2	a	L12R0	373.52	–
		L12R15	298.67	–
		L12R30	200.01	–
	b	L12W0	411.32	10.12
		L12W15	326.19	9.21
		L12W30	210.80	5.39
	c	L6W0	397.53	6.43
		L6W15	309.89	3.76
		L6W30	205.23	2.61

be considered as a reference for the other two columns in the same category. Thus, the decrements in ultimate load for $e/t=0.13$ and $e/t=0.26$ were 27% and 50%, respectively, based on the average decrements of the six categories.

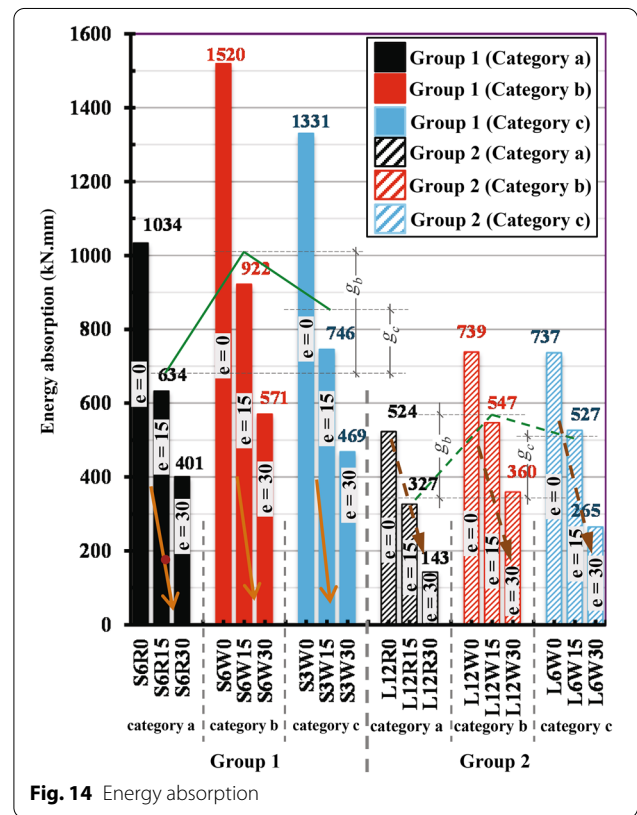
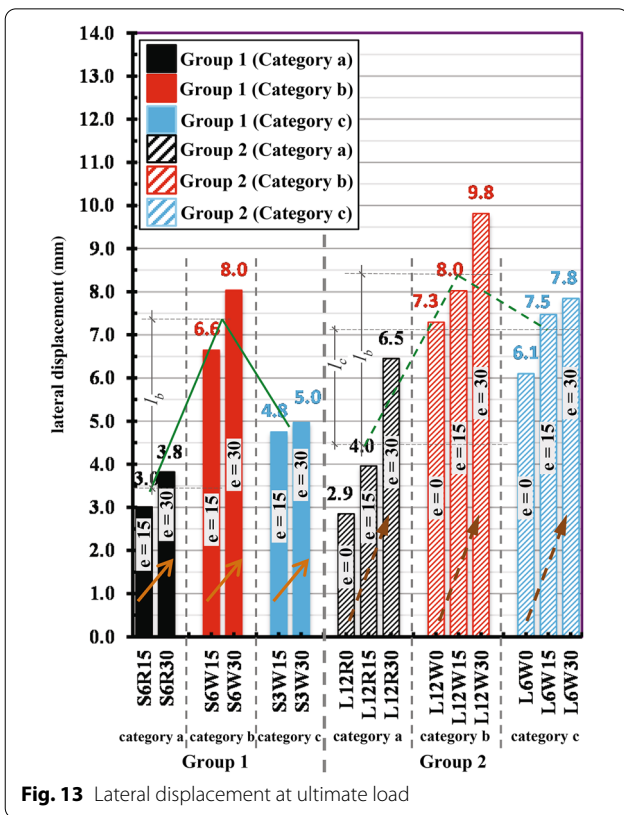
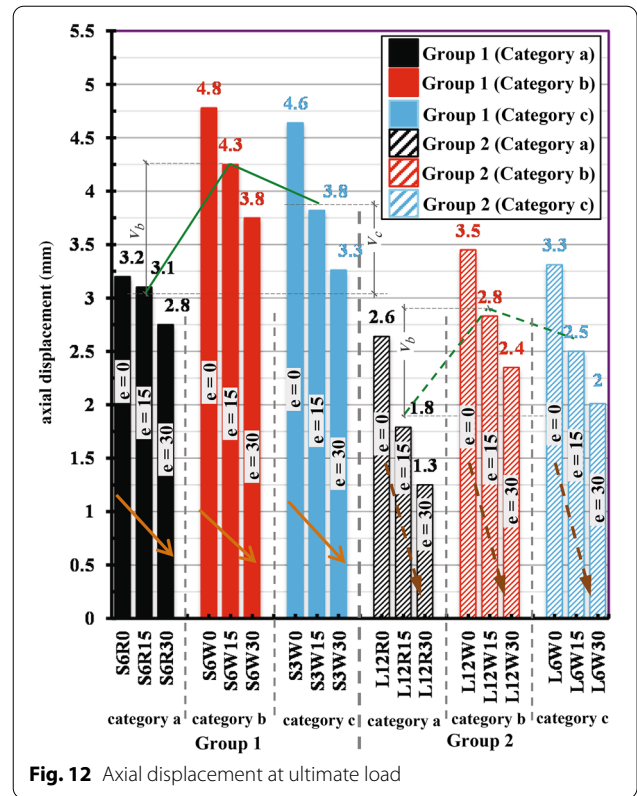
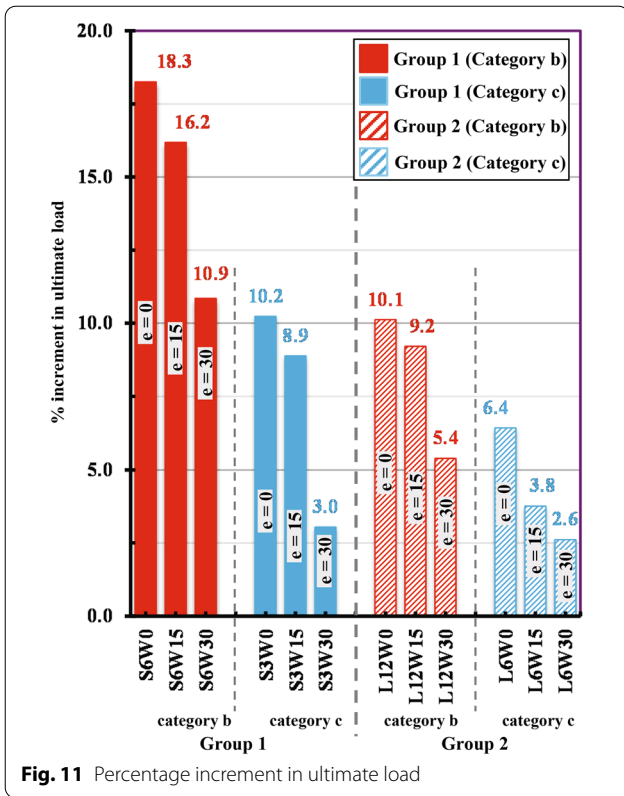
The results of the short concentrically and eccentrically loaded column specimens (S6R0, S6W0, and S6W15) could be compared with the similar studies in the literature review (El-Kholy & Dahish 2015; El-Kholy et al. 2018; Hadi & Zhao 2011; Tahir et al. 2017). These studies and the current study could be sorted in ascending order according to the maximum improvement in ultimate load as follows; (1) El-Kholy and Dahish (2015) gained 11.02% improvement, (2) Hadi and Zhao (2011) gained 13.05% improvement, (3) Tahir et al. (2017) gained 17.93% improvement, (4) the current study gained 18.3% improvement, and finally (5) El-Kholy et al. (2018) gained 35.43% improvement. The smaller improvements gained by the first three studies compared with the others were ascribed to using EMM (the first and third studies) or weak WWM (the second study). The outperformance of Tahir et al. (2017)



study over El-Kholy and Dahish (2015) in terms of the ultimate load improvement was attributed to its higher ρ (0.76%) and the smaller λ (4.9). In addition, both the simulated ideal pinned boundary conditions and used high strength concrete by Hadi and Zhao (2011) reduced the contribution of the utilized weak WWM to the ultimate improvement. Using strong WWM increased the ultimate load improvement of both the current study and El-Kholy et al. (2018). The simulated ideal pinned boundary conditions for a relatively higher λ (9) in the current study minimized the WWM improvement to the ultimate load compared with El-Kholy et al. (2018) study in which fixed boundary conditions was simulated for a smaller λ of 7.3. It is worth reminding that there are no previous studies that used metal meshes (WWM or other types) for long columns under either concentric or eccentric compression, and there is only one study (Hadi & Zhao 2011) that used WWM for short columns under eccentric compression. Thus, the results of the current study could not be related to more previous studies.

3.2 Deformation

Fig. 10 illustrates the load–deformation histories for categories a, b, and c with black, red, and cyan colors, respectively. Figs. 10, 11, 12, 13 and 14 reveal that the most ductile category (higher deformations and higher energy absorption) was b followed by c, and finally the reference a for the same eccentricity ratio. It could be argued that the outperformance of both categories b and c over category a was due to the use of WWM. However, the outperformance of category b over c was due to the use of ties with higher ρ ($\rho_r = 0.44$). Figs. 12, 13 and 14 confirm that adding one layer of WWM as an internal reinforcement to the transverse steel ties (with ratio of either ρ_r or $0.5\rho_r$) increased both the deformation (either axial or lateral) and the energy absorption for all columns. For category b (ρ_r ties), the average increments in axial displacement (v_b), lateral displacement (l_b), and energy absorption (g_b) were 47%, 101%, and 56% according to Figs. 12, 13 and 14 respectively. For category c ($0.5\rho_r$ ties), the average increments in axial displacement (v_c), lateral displacement (l_c), and energy absorption (g_c) were reduced to 33%, 52%, and 39%, respectively.



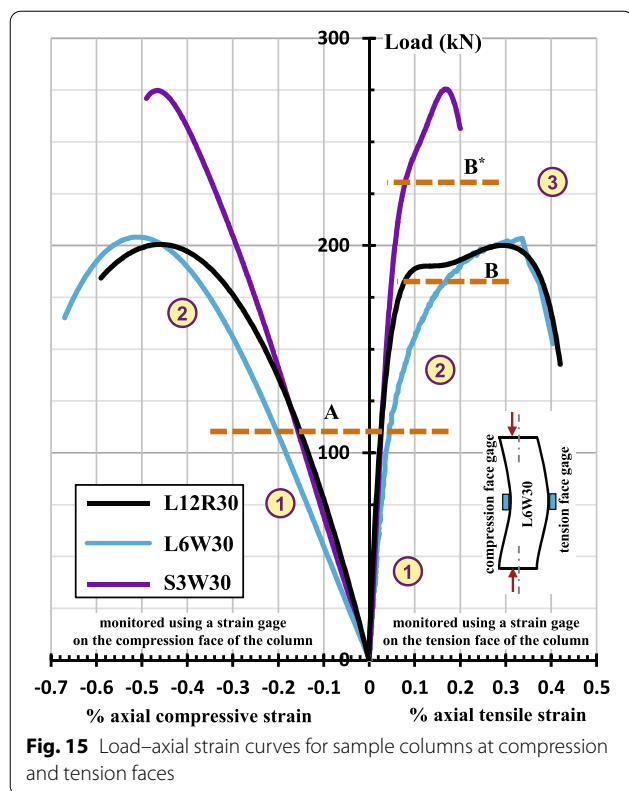


Fig. 15 Load-axial strain curves for sample columns at compression and tension faces

Also, it was observed that increasing the λ at the same e/t or increasing e/t at the same λ , decreased both the axial deformation (Fig. 12) and the energy absorption (Fig. 14) but increased the lateral deformation (Fig. 13). The decrement in axial displacement was ascribed to the reduction in the ultimate load, whereas the increment in the lateral displacement was ascribed to the transformation of the failure mode from compression to flexure. Comparing the v , g , and l values of short columns with the corresponding values of long columns in Figs. 12, 13 and 14, respectively, confirmed the effect of λ on reducing the axial deformation, reducing the energy absorption, and increasing lateral deformation. In other words, the average axial displacement and the average energy absorption of long columns were reduced by 21% and 16%, respectively, compared with those of the corresponding short columns. In contrast, the average lateral displacement of long columns was increased by 22% compared with short columns. For the effect of e/t , the inclined arrows direction in Figs. 12, 13 and 14 emphasized the effect of increasing e/t on reducing the axial deformation, reducing the energy absorption, and increasing the lateral deformation, respectively. The slope of inclined arrows (Figs. 12, 13 and 14) revealed the combined effects of increasing both e/t and λ . For example, the reduction

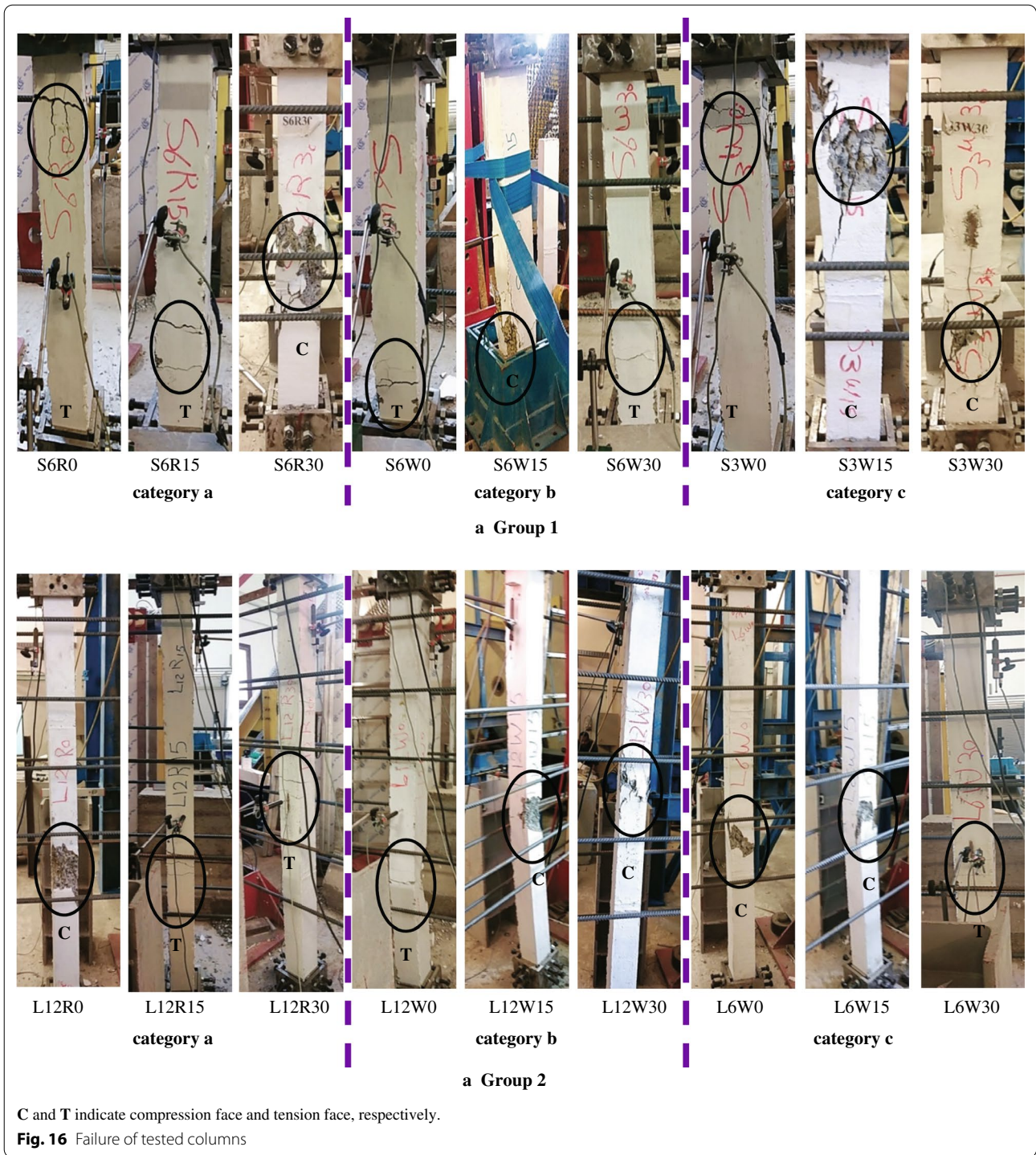
rate in axial displacement due to the increase in e/t (from zero to 0.26) was slightly higher for long columns than short columns (Fig. 12). In addition, the increment rate in lateral displacement due to the increase in e/t was a bit higher for long columns than short columns (Fig. 13). However, the decrement rate in energy absorption due to the increase in e/t was steep and approximately equal for both short and long columns (Fig. 14). This steep reduction in energy absorption in all categories (average 36% and 63% for $e/t=0.13$ and 0.26, respectively) was attributed to the steep reduction rate in the ultimate load with increasing eccentricity (Table 6 and “Ultimate load”).

Although the exact definition of ductility is still debatable issue in field of engineering (Yaqub et al. 2013), ductility might be explained as the ability of RC column to undergo considerable plastic deformation without failure (El-Kholy et al. 2022). The improvement in ductility could be expressed by comparing the deformation of the different column specimens (El-Kholy et al. 2022) or correlated to the energy absorption of each specimen (Emara et al. 2021; Hadi 2007). Based on the deformation and energy absorptions values in the current study, it was shown in this section that the columns comprising ρ_r ties and a WWM layer (category b) gained the highest improvement in ductility. Then, the columns comprising $0.5\rho_r$ ties and a WWM layer (category c) showed a relatively smaller improvement in ductility. In addition, it was shown that the ductility was reduced by increasing the slenderness ratio and the eccentricity ratio.

3.3 Axial Strain

Fig. 15 shows the load-%axial strain histories at mid-height of the column on the compression and tension faces for three sample columns (S6R30, L12R30, and L6W30) tested under 30 mm eccentricity ($e/t=0.26$). For the compression face, the load-compressive strain relationship might be idealized as bilinear. In its first interval, the increase rate of compressive strain was higher for long columns comprising a WWM layer (L6W30) than the reference column (L12R30) because of the additional ductility contributed by the WWM layer. The second interval started at level A (40% and 55% of the ultimate load for the short and long columns, respectively). This interval was characterized with a greater increase rate in the strain for the three columns indicating significant flexural and nonlinear behavior. This greater rate was more evident for the long columns (L12R30 and L6W30) that exhibited noticeable buckling.

On the tension face of the sample columns, the load-tensile strain history showed a trilinear relationship. In the first interval, the increase rate in tensile strain was too small. This could be attributed to the neutralization of the compressive strain resulting from the compression load



with the significant tensile strain resulting from the flexural deformation due to a 30 mm eccentricity. In case of smaller eccentricity values, an initial compressive strain with a decreasing rate might be monitored on the tension face before it turned into a tensile strain (El-Kholy et al. 2019b). The second interval started from level A to level

B and B^{*} for long and short columns, respectively. This interval was characterized by a noticeable flexural deformation causing significant tensile strain that overcame the compressive strain of the vertical load. The increase rate of the tensile strain was higher for the long columns and especially L6W30 due to the existence of WWM. The

third interval started from level B for long columns (91% of ultimate load) and level B* for short columns (84% of ultimate load). In this last interval, the tensile strain was characterized with successive increments showing a high increase rate for long columns and a relatively smaller rate for short columns till failure.

3.4 Cracks and Failure

Fig. 16 shows the failure patterns of the investigated columns. The failure in all columns was flexural because of the eccentricity of load, the ideal pinned boundary conditions, and the high slenderness ratio especially for group 2 ($\lambda = 18$). For group 1, the flexural failure was characterized with a larger crushed area (compared with group 2) of the concrete cover on the compression face of the specimen. This observation was more evident for zero eccentricity specimens. This large crushed part of concrete cover could be ascribed to the higher axial load (compressive stress) sustained by group 1 (short columns), and therefore reaching the confinement capacity.

The ideal hinged simulated by the steel caps (Fig. 8) assured free rotations at both ends. These ideal boundary conditions magnified the overall buckling behavior, increased the flexural stresses on the compression and tension faces of the columns. For the reference columns (comprising traditional reinforcement of longitudinal bars and ρ_r ties), the failure was sudden, brittle, and accompanied by a bang noise. In addition, the first crack was observed at approximately 77% of ultimate load, and no significant deformation was monitored before failure. For the columns with an additional internal reinforcement of WWM, the structural behavior was more ductile, and noticeable deformation (overall buckling) could be seen first. Then, tension cracks were initiated at approximately 90% of the ultimate load. Finally, compression cracks were recorded, and failure occurred. The failure noise was relatively low compared with the reference columns. The previous observations were more evident for the eccentrically loaded columns than concentrically loaded columns.

4 Conclusions

This study was conducted with the aim of investigating the effectiveness of using a WWM layer as an additional internal reinforcement to the traditional steel reinforcement consisting of longitudinal bars and transverse ties ($\rho = 0.44\%$ and 0.22%) for short columns ($\lambda = 9$) and long columns ($\lambda = 18$) under concentric and eccentric compression ($e/t = 0.13$ and 0.26). The following conclusions could be drawn based on the analysis of the experimental results.

1. Adding one layer of WWM as an internal reinforcement to the traditional steel reinforcement with ties of $\rho_r = 0.44\%$ increased the ultimate load by 15% and 8% for short and long columns, respectively.
2. Reducing ρ_r to half the reference value ($\rho = 0.22\%$) reduced the ultimate load improvements to approximately half the percentages introduced in item 1.
3. The improvement in ultimate load for long columns was approximately half that of short columns and was more significant for concentric load than eccentric load.
4. The highest ductility was shown by the columns comprising a WWM layer and ρ_r ties followed by those comprising a WWM layer and $0.5\rho_r$ ties compared with reference columns that had no WWM layers.
5. The maximum compressive and tensile strains on the two faces (that were under extreme flexural deformation) of the column were higher for the long columns compared with short columns.
6. The increase rates of the compressive and tensile strains were higher for the columns comprising a WWM layer compared with the reference columns.
7. The WWM layer mitigated the failure noise and provided a warning ample in a form of significant deformation before failure unlike columns with traditional reinforcement, where the failure was sudden, brittle, and accompanied by a bang noise.
8. The crushed area of concrete cover was larger for short columns than long columns because of the combined effect of the higher axial stress and the flexural stress.

Author Contributions

AME proposed the research point (conceptualization and methodology), designed the experimental plan, designed the test setup, supervised the preparation and testing phases, analyzed the results, prepared the figures, and wrote the paper. In addition, AME was responsible for submission, correspondence with the journal, and preparing the revised paper.

SFA prepared the specimens, and prepared the steel caps, tested the materials, tested the specimens, prepared the draft charts, prepared the results, and shared in writing the draft paper.

MMA Supervision, reviewed the research plan, reviewed the test setup, and reviewed the paper.

All authors read and approved the final manuscript.

Author Information

Ahmed M. El-Kholy is an associate professor of Structural Engineering at Department of Civil Engineering at Fayoum University, Egypt. His research interests include nonlinear finite element analysis, finite element modeling, failure analysis, imperfection modeling, RC columns, multistory buildings, seismic analysis, seismic codes, masonry infilled RC frames, and nontraditional materials for construction of new structures and repair of existing structures.

Safaa F. Abd El-Rahman is a teaching assistant of Structural Engineering at Department of Civil Engineering at Nahda University (NUB), Beni Suef, Egypt. Engineer Safaa is a Master student at Fayoum University, Egypt. Her research interests include RC columns and nontraditional materials for construction of new structures and repair of existing structures.

Mohamed M. El-Assaly is a professor and the head of Structural Engineering at Department of Civil Eng. at Fayoum University, Egypt. Professor El-Assaly is the vice dean for education and student affairs at the faculty of Eng., Fayoum U. In addition, he was the head of Structural Engineering Consulting Office at Fayoum U. His research interests include finite element analysis, earthquake Engineering, seismic analysis and design, RC structures, and repair of RC structures.

Funding

Open access funding provided by The Science, Technology & Innovation Funding Authority (STDF) in cooperation with The Egyptian Knowledge Bank (EKB).

Availability of Data and Materials

Not applicable.

Declarations

Competing Interests

The authors declare that they have no competing interests.

Author details

¹Civil Engineering Department, Faculty of Engineering, Fayoum University, Kiman Fares, El-Fayoum, Egypt. ²Civil Engineering Department, Faculty of Engineering, Nahda University (NUB), Beni Suef, Egypt.

Received: 26 April 2022 Accepted: 3 October 2022

Published online: 15 February 2023

References

- Abd El-Rahman, S. (2022). *Effectiveness of New Lateral Reinforcement for RC Columns (Short and Long) Under Concentric and Eccentric Loadings*. MSc Thesis. Supervisors: M. El-Assaly & A. EL-Kholy. Fayoum (Egypt): Fayoum University
- ACI Committee 318. (2014). *ACI 318–14 Building Code Requirements for Structural Concrete and Commentary*. MI (USA): American Concrete Institute (ACI)
- Al-Nimry, H., & Al-Rabadi, R. (2019). Axial-Flexural Interaction in FRP-Wrapped RC Columns. *International Journal of Concrete Structures Materials*, 13, 53. <https://doi.org/10.1186/s40069-019-0366-8>
- Al-Nimry, H., & Ghanem, A. (2017). FRP Confinement of Heat-Damaged Circular RC Columns. *International Journal of Concrete Structures Materials*, 11(1), 115–133. <https://doi.org/10.1007/s40069-016-0181-4>
- Bastami, M., Mousavi, A., & Abbasnejadfar, M. (2022). Evaluation of mechanical characteristics of high-strength reinforced concrete columns with hexagonal chicken wire mesh under cyclic loading. *International Journal of Concrete Structures Materials*, 16, 30. <https://doi.org/10.1186/s40069-022-00520-0>
- Choi, D., Hong, S., Lim, M., Ha, S., & Vachirapanyakun, S. (2021). Seismic retrofitting of RC circular columns using carbon fiber, glass fiber, or ductile PET fiber. *International Journal of Concrete Structures Materials*, 15, 46. <https://doi.org/10.1186/s40069-021-00484-7>
- CMB—Chemicals for Modern Buildings. (2013). *Technical data sheet of release agent—ZETOLAN SH2*. Cairo (Egypt): CMB
- Daou, A., Chehab, G., Saad, G., & Hamad, B. (2020). Experimental and numerical investigations of reinforced concrete columns confined internally with biaxial geogrids. *Construction and Building Materials*, 263, 120115. <https://doi.org/10.1016/j.conbuildmat.2020.120115>
- Egyptian Standards—Building Materials Committee. (2008). *Aggregates for Concrete—ES 1109*. Cairo (Egypt): Egyptian Organization for Standards and Quality (EOS).
- Egyptian Standards—Building Materials Committee. (2009). *Cement Part1: Composition, specifications and conformity criteria for common cements—ES 4756–1*. Cairo (Egypt): Egyptian Organization for Standards and Quality (EOS).
- Egyptian Code Committee for Concrete Structures. (2018). *Egyptian code for design and construction of concrete structures—ECP 203–2018*. Giza (Egypt): Housing and Building National Research Center (HBRC).
- Egyptian Standards—Ferrous Products Committee. (2015a). *Steel for the Reinforcement of Concrete Part 1: Plain Bars—ES 262–1*. Cairo (Egypt): Egyptian Organization for Standards and Quality (EOS).
- Egyptian Standards—Ferrous Products Committee. (2015b). *Steel for the Reinforcement of Concrete Part 2: Ribbed Bars—ES 262–2*. Cairo (Egypt): Egyptian Organization for Standards and Quality (EOS).
- El Maaddawy, T. (2009). Strengthening of eccentrically loaded reinforced concrete columns with fiber-reinforced polymer wrapping system experimental investigation and analytical modeling. *Journal of Composites for Construction*, 13(1), 13–24. [https://doi.org/10.1061/\(ASCE\)1090-0268\(2009\)13:1\(13\)](https://doi.org/10.1061/(ASCE)1090-0268(2009)13:1(13))
- El-Kholy, A., Abd El-Mola, S., Abd, E.-A., & Shaheen, A. (2018). Effectiveness of combined confinement with metal meshes and ties for preloaded and post-heated RC short columns. *Arabian Journal for Science and Engineering*, 43, 1875–1891. <https://doi.org/10.1007/s13369-017-2782-x>
- El-Kholy, A., & Dahish, H. (2015). Improved confinement of reinforced concrete columns. *Ain Shams Engineering Journal*, 7(2), 717–728. <https://doi.org/10.1016/j.asej.2015.06.002>
- El-Kholy, A., Masaoud, M., & Abd El-Aziz, M. (2019a). Enhanced ferrocement jackets for strengthening long reinforced columns. *International Journal of Civil Engineering and Technology*, 10(8), 61–72.
- El-Kholy, A., Mourad, S., Shaheen, A., & Mohammed, Y. (2019b). Finite element simulation for steel tubular members strengthened with FRP under compression. *Structural Engineering and Mechanics*, 72(5), 569–583. <https://doi.org/10.12989/sem.2019.72.5.569>
- El-Kholy, A., Osman, A., & El-Sayed, A. (2022). Nonlinear finite element analysis of slender RC columns strengthened with FRP sheets using different patterns. *Computers and Concrete*, 29(4), 219–235. <https://doi.org/10.12989/cac.2022.29.4.219>
- Emara, M., Mohamed, H., Rizk, M., & Hu, J. (2021). Behavior of ECC columns confined using steel wire mesh under axial loading. *Journal of Building Engineering*. <https://doi.org/10.1016/j.jobee.2021.102809>
- Gajdosova, K., & Bilcik, J. (2013). Full-scale testing of CFRP-strengthened slender reinforced concrete columns. *Journal of Composites for Construction*, 17(2), 239–248. [https://doi.org/10.1061/\(ASCE\)CC.1943-5614.0000329](https://doi.org/10.1061/(ASCE)CC.1943-5614.0000329)
- Ganesan, N., & Anil, J. (1993). Strength and behavior of reinforced concrete columns confined by ferrocement. *Journal Ferrocement*, 23(2), 99–108.
- Ghanem, S., & Harik, I. (2018). Concentrically Loaded Circular RC Columns Partially Confined with FRP. *International Journal of Concrete Structures and Materials*, 12, 52. <https://doi.org/10.1186/s40069-018-0283-2>
- Hadi, M. (2007). Behaviour of FRP strengthened concrete columns under eccentric compression loading. *Composite Structures*, 77(1), 92–96. <https://doi.org/10.1016/j.compstruct.2005.06.007>
- Hadi, M., & Zhao, H. (2011). Experimental study of high-strength concrete columns confined with different types of mesh under eccentric and concentric loads. *Journal of Materials in Civil Engineering*, 23(6), 823–832. [https://doi.org/10.1061/\(ASCE\)MT.1943-5533.0000234](https://doi.org/10.1061/(ASCE)MT.1943-5533.0000234)
- Hashemi, N., Hassanpour, S., & Oskoei, A. (2022). The effect of rebar embedment and CFRP confinement on the compressive strength of low-strength concrete. *International Journal of Concrete Structures and Materials*, 16, 17. <https://doi.org/10.1186/s40069-022-00502-2>
- Kaish, A., Jamil, M., Raman, S., Zain, M., & Nahar, L. (2018). Ferrocement composites for strengthening of concrete columns: A review. *Construction and Building Materials*, 160, 326–340. <https://doi.org/10.1016/j.conbuildmat.2017.11.054>
- Pan, J., Xu, T., & Hu, Z. (2007). Experimental investigation of load carrying capacity of the slender reinforced concrete columns wrapped with FRP. *Construction and Building Materials*, 21(11), 1991–1996. <https://doi.org/10.1016/j.conbuildmat.2006.05.050>
- Quiertant, M., & Clement, J. (2011). Behavior of RC columns strengthened with different CFRP systems under eccentric loading. *Construction and Building Materials*, 25(2), 452–460. <https://doi.org/10.1016/j.conbuildmat.2010.07.034>

- Raval, R., & Dave, U. (2013). Behavior of GFRP wrapped RC columns of different shapes. *Procedia Engineering*, 51, 240–249. <https://doi.org/10.1016/j.proeng.2013.01.033>
- Razvi, S., & Shaikh, M. (2018). Effect of confinement on behavior of short concrete column. *Procedia Manufacturing*, 20, 563–570. <https://doi.org/10.1016/j.promfg.2018.02.084>
- Si Youcef, Y., Amziane, S., & Chemrouk, M. (2015a). CFRP confinement effectiveness on the behavior of reinforced concrete columns with respect to buckling instability. *Construction and Building Materials*, 81, 81–92. <https://doi.org/10.1016/j.conbuildmat.2015.02.006>
- Si Youcef, Y., Amziane, S., & Chemrouk, M. (2015b). Effectiveness of strengthening by CFRP on behavior of reinforced concrete columns with respect to the buckling instability. *Materials and Structures*, 48, 35–51. <https://doi.org/10.1617/s11527-013-0166-6>
- Siddiqui, N., Abbas, H., Almusallam, T., Binyahya, A., & Al-Salloum, Y. (2020). Compression behavior of FRP-strengthened RC square columns of varying slenderness ratios under eccentric loading. *Journal of Building Engineering*, 32, 101512. <https://doi.org/10.1016/j.jobbe.2020.101512>
- Tahir, M., Khan, Q., Shabbir, F., Ijaz, N., & Malik, A. (2017). Performance of RC columns confined with welded wire mesh around external and internal concrete cores. *Technical Journal UET Taxila*, 22(1), 8–16.
- Vesmawala, G., & Kodag, P. (2017). Investigation of GFRP strengthened RC non-slender columns under eccentric loading. *Građevinar*, 69(9), 831–840. <https://doi.org/10.14256/JCE.1591.2016>
- Widiarsa, I., & Hadi, M. (2013). Performance of CFRP wrapped square reinforced concrete columns subjected to eccentric loading. *Procedia Engineering*, 54, 365–376. <https://doi.org/10.1016/j.proeng.2013.03.033>
- Xing, L., Lin, G., Chen, J. F. (2020) Behavior of FRP-Confined Circular RC Columns under Eccentric Compression. *Journal of Composites for Construction*, 24(4), 04020030. [https://doi.org/10.1061/\(ASCE\)CC.1943-5614.0001036](https://doi.org/10.1061/(ASCE)CC.1943-5614.0001036)
- Yaqub, M., Bailey, C., Nedwell, P., Khan, Q., & Javed, I. (2013). Strength and stiffness of post-heated columns repaired with ferrocement and fiber reinforced polymer jackets. *Composites Part B: Engineering*, 44(1), 200–211. <https://doi.org/10.1016/j.compositesb.2012.05.041>

Publisher's Note

Springer Nature remains neutral with regard to jurisdictional claims in published maps and institutional affiliations.

Submit your manuscript to a SpringerOpen[®] journal and benefit from:

- Convenient online submission
- Rigorous peer review
- Open access: articles freely available online
- High visibility within the field
- Retaining the copyright to your article

Submit your next manuscript at ► [springeropen.com](https://www.springeropen.com)
